JOURNAL OF PROPULSION AND POWER
Vol. 27, No. 1, January–February 2011

Driver Gas Reduction Effect of Pulse-Detonation-Engine Initiator Using Reflecting Board

Masashi Wakita,* Ryusuke Numakura,† Takatoshi Asada,‡ Masayoshi Tamura,§
Tsuyoshi Totani,¶ and Harunori Nagata**
Hokkaido University, Hokkaido 060-8628, Japan

DOI: 10.2514/1.50043

To reduce driver gas usage of a pulse detonation engine operating in airbreathing mode, the authors experimentally examined a combination method of a reflecting board and overfilling of the driver gas. This method has the potential to reduce the predetonator diameter by half and shorten the overfilling distance h to the reflecting board position w. Experiments with stoichiometric hydrogen–oxygen and hydrogen–air mixtures as driver and target gases, respectively, showed that the overfilling distance necessary to have a planar detonation wave propagate in a detonation chamber is reduced to 30 mm when a reflecting board is used with a reflecting board clearance of $w = 10$ mm. With an overfilling distance of 30 mm, the transformation of the detonation wave from cylindrical to toroidal did not occur because of the mixing effect of the driver gas and the target gas around the reflecting board. A 100-mm-thick reflecting board prevents the mixing effect, and a successful transformation from cylindrical to toroidal becomes possible with an overfilling distance as small as 17.2 mm.

Introduction

A PULSE detonation engine (PDE), in which propellant burns in detonation waves intermittently, has attracted the attention of researchers because of its simplicity and theoretical higher thermal efficiency [1–4]. The major issue that needs to be resolved for the practical use of a PDE is detonation initiation. Detonability is an indicator of the ease of initiating detonation of combustible mixtures. When a PDE operates in airbreathing mode, the combustible gas is likely to be a fuel–air mixture, and its detonability (meaning detonation initiation ability of the combustible mixture) is lower than that of fuel–oxygen mixtures [5]. Another case in which one may encounter a low-detonability condition is when the fuel is in the liquid phase. The energy required to initiate detonation with low-detonability propellants, such as those mentioned previously, is too large to directly initiate a detonation wave using a typical energy source [4].

To initiate a detonation wave using a typical energy source, many researchers employ a deflagration-to-detonation transition (DDT) process. Unfortunately, a low-detonability combustible mixture needs both a long distance and time for the DDT process, resulting in a decrease in operating frequency and thermal efficiency. Many researchers have succeeded in reducing the DDT length and time by using vortex generators, such as a Shchelkin spiral, in an upstream region of the detonation chamber. However, vortex generators in a detonation chamber can cause nonrepeatable ignition due to a temperature increase during operation.

Another possible method of detonation initiation is the predetonator concept. It is common knowledge that the smaller the diameter of a tube, the more easily a detonation wave can be initiated. As Fig. 1a shows, the predetonator concept uses a two-step detonation initiation process. A detonation wave readily commences in a small diameter tube (predetonator) using a low-energy source. To reduce the DDT length, a high-detonability mixture of propellants is often added as a driver gas to the upstream region of the predetonator. In the next stage, the detonation wave transmits into a larger-diameter detonation chamber containing a low-detonability mixture of propellants (target gas) [4]. Detonation transition through an abrupt area change, such as from the predetonator to the main chamber, is of foremost interest in the field of fundamental detonation study, and there have been many investigations concerning this issue [6–9]. Mitrofanov and Soloukhin have shown that the tube diameter $\boldsymbol{d}$ must be at least 13 times the cell size $\boldsymbol{\lambda}$ for a successful detonation transition [10]. Matsui and Lee proposed the critical tube diameter concept, meaning that the tube diameter $\boldsymbol{d}_c$ under this marginal condition represents detonability [11]. Knystautas et al. obtained $\boldsymbol{d}_c$ values of various combustible mixtures and showed that the relation of $\boldsymbol{d}_c = 13\boldsymbol{\lambda}$ is valid for various mixtures [12]. However, many subsequent experimental studies showed that $\boldsymbol{d}_c = 13\boldsymbol{\lambda}$ does not work out, which has been well reviewed in [13]. Moen et al. found that $\boldsymbol{d}c/\boldsymbol{\lambda}$ ranges from 13 to 24 for fuel–air mixtures [14]. Many researchers have demonstrated that $\boldsymbol{d}_c$ varies between $4\boldsymbol{\lambda}$ and $30\boldsymbol{\lambda}$, depending on the type and concentration of the diluent [15–18].

Most of the initiators use a driver gas mixture in the uppermost part of the tube, as Fig. 1a shows. Typical compositions of a driver gas mixture are hydrogen–oxygen and ethylene–oxygen. The short DDT length (or time) of these mixtures allows for an extremely short predetonator. Using a driver gas mixture improves the ignition probability and reliability of a PDE system. However, the additional oxygen in the driver gas means an increase in the onboard propellant weight and reduces I_{sp} of the PDE system. Recent performance analyses by Aamio et al. [19] and Brophy et al. [20] have shown that a driver gas accounting for only 1% of the total combustion chamber volume results in a 22% reduction in I_{sp}. Accordingly, we must keep the driver gas usage as small as possible. Because the amount of the driver gas is proportional to the sectional area of the predetonator, I_{sp} increases as the diameter of the predetonator decreases.

Many methods to enhance the detonation transition at the abrupt change of area have been proposed. Typical methods are the use of

Received 25 March 2010; revision received 2 July 2010; accepted for publication 26 August 2010.

*Assistant Professor, Graduate School of Engineering, Division of Mechanical and Space Engineering, North 13, West 8, Kita-ku, Sapporo; m-wakita@eng.hokudai.ac.jp. Member AIAA.

†Ph.D. Student, Graduate School of Engineering, Division of Mechanical and Space Engineering, North 13, West 8, Kita-ku, Sapporo.

‡Graduate Student, Graduate School of Engineering, Division of Mechanical and Space Engineering, North 13, West 8, Kita-ku, Sapporo.

§Graduate Student, Graduate School of Engineering, Division of Mechanical and Space Engineering, North 13, West 8, Kita-ku, Sapporo; t-masa@mech-hm.eng.hokudai.ac.jp.

¶Associate Professor, Graduate School of Engineering, Division of Mechanical and Space Engineering, North 13, West 8, Kita-ku, Sapporo; tota@eng.hokudai.ac.jp. Member AIAA.

**Professor, Graduate School of Engineering, Division of Mechanical and Space Engineering, North 13, West 8, Kita-ku, Sapporo; nagata@eng.hokudai.ac.jp. Member AIAA.

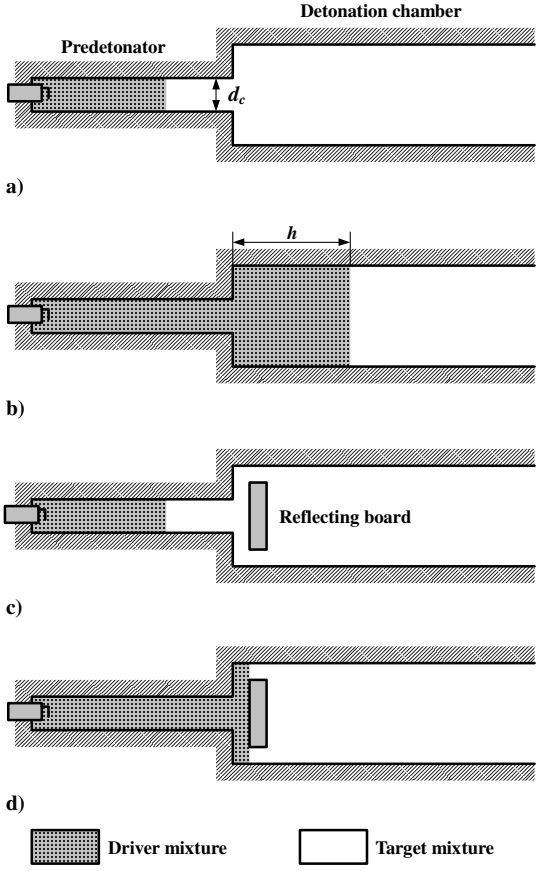

Fig. 1 Concept of reflecting board and overfilling of driver.

1) shock reflection and shock-focusing devices and 2) a cone-shaped exit having a gradual area change to reduce lateral expansion. An example of detonation transition enhancement using the concentration of shock wave reflection and focusing is the experimental research of Moen et al. [21]. They showed that an annular orifice at a predetonator exit enhances the detonation transition, and the most efficient blockage ratio (BR) (equal to the obstacle surface area divided by the predetonator cross section) was around 0.5. By using an annular orifice of BR $= 0.5$ at the predetonator exit, the critical tube diameter $\boldsymbol{d}_c$ is reduced to $5.7\boldsymbol{\lambda}$–$7\boldsymbol{\lambda}$. Sorin et al. installed an inversed intermediate single-ended tube at the predetonator exit and provided a critical tube diameter of $2.2\boldsymbol{\lambda}$ for a double-shock reflection [22]. As an example of a cone-shaped exit, Khasainov et al. showed that a cone-shaped exit with a half angle of less than 45 deg enhances the detonation transition [23]. The critical tube diameter decreases linearly with the angle from $13\boldsymbol{\lambda}$ to $1\boldsymbol{\lambda}$.

The critical diameter of the predetonator is determined by the cell size of the target gas mixture. An effective method to reduce the diameter of the predetonator is to overfill the driver gas over the predetonator exit area, as Fig. 1b shows. In this method, the cell size of the driver gas mixture determines the diameter of the predetonator. Because the cell size of the driver gas mixture is usually one to two orders of magnitude smaller than that of the target gas mixture [5], we can reduce the predetonator diameter according to the scale ratio of the cell sizes. Accordingly, a drastic reduction in the predetonator volume, in comparison with the other enhancement devices mentioned previously, is possible using this method. On the other hand, minimization of the overfilling distance $\boldsymbol{h}$, in Fig. 1b, arises as another challenge to reducing driver gas usage.

To realize a successful transition of detonation at the predetonator exit in a PDE operating in airbreathing mode, in which the combustible gas is a fuel–air mixture, the authors also have proposed a PDE initiator that uses a reflecting board near the exit of the predetonator tube, as Fig. 1c shows [24,25]. Figure 2 shows an overall photograph of a PDE initiator with a reflecting board. In these studies, the authors

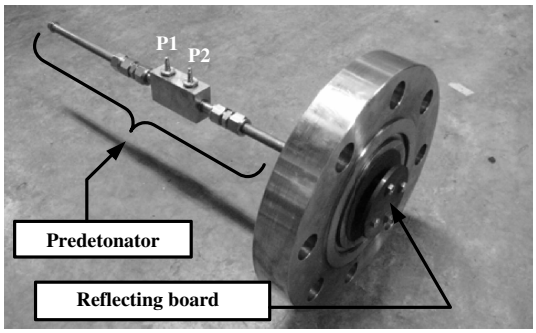

Fig. 2 PDE initiator with reflecting board.

showed that the minimum diameter of the predetonator with a reflecting board is expressed by $\boldsymbol{d}_c = 6.3\boldsymbol{\lambda}$.

In this study, the authors propose a combination method that uses a reflecting board and overfilling of the driver gas to reduce the driver gas usage of a PDE initiator. This method has the potential to reduce the predetonator diameter by half and shorten the overfilling distance $\boldsymbol{h}$ to the reflecting board position $\boldsymbol{w}$, as Fig. 1d shows. This study consisted of two steps. In the first step, we developed a preliminary design based on our previous work and made a performance evaluation. The second step was an experimental investigation into the driver gas reduction ability of this method.

Pulse-Detonation-Engine Initiator with Reflecting Board

Outline of Pulse-Detonation-Engine Initiator with Reflecting Board

Teodorczyk et al. analyzed a quasi-detonation wave propagating in an obstacle-laden channel and showed that Mach reflections at a rigid wall play an important role in detonation propagation [26]. Jones et al. showed numerical results in which a detonation wave entering a wide channel from a narrow tube decayed once and then recommenced owing to a Mach reflection at the sidewall of the channel [27]. Ohyagi et al. observed this phenomenon experimentally [28]. Murray and Lee [29] and Murray et al. [30] studied transitions of a planar detonation wave from a circular tube to a cylindrical detonation expanding radially outward between a pair of parallel plates, and they showed that a Mach reflection of a diffracted wave from the wall opposing the tube exit promotes the transition of detonation. De Witt et al. investigated detonation initiation via the interaction of a high-speed shock/flame complex and a disk or a cone obstacle placed in the middle of the detonation chamber [31].

Inspired by these results, the authors have proposed a PDE initiator using a circular disk called a reflecting board near the exit of a predetonator to promote detonation transition by Mach reflection on the board [23]. To evaluate the performance of this PDE initiator, the authors conducted experiments using the configuration shown in Fig. 3. The predetonator diameter $\boldsymbol{d}$, the diameter of the detonation chamber $\boldsymbol{D}$, and the gap of the annular path $\boldsymbol{L}$ are 20, 100, and 15 mm, respectively. Combustible gases were stoichiometric hydrogen–oxygen mixtures diluted with nitrogen or argon. There is no composition change from the predetonator to the detonation chamber. The initial pressure was 1 standard atmosphere (atm). We determined critical values for the cell size $\boldsymbol{\lambda}$ for successful transitions with various reflecting board distances by changing the concentration of the dilution gas. The critical value of the cell size $\boldsymbol{\lambda}$ correlates

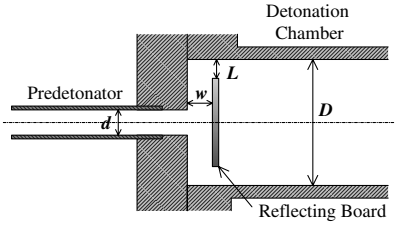

Fig. 3 Test section.

strongly with the dimensions of the predetonator, and the threshold limit value of d/λ for a successful transition is 13 without a reflecting board. We have confirmed that a reflecting board at the appropriate position improves the threshold limit value of the d/λ to 6.3. Accordingly, the reflecting board reduces the predetonator diameter by one half.

A detonation wave propagates around the reflecting board, changing its shape through three transition processes, as Fig. 4 shows. The first transition process is from a planer detonation wave in the predetonator (Fig. 4a) to an expanding cylindrical detonation wave between the front flange surface and the reflecting board (Fig. 4b). The second transition process occurs on the sidewall of the detonation chamber with which the expanding cylindrical detonation wave collides. This collision converts the wave into a imploding toroidal detonation wave (Fig. 4c). The third transition process occurs in the rearward region of the reflecting board through the implosion of the imploding toroidal detonation wave. The wave implosion causes a reinitiation of a spherical detonation wave, which becomes a planar detonation wave in the downstream of the detonation chamber (Fig. 4d). Many researchers have performed experimental or numerical studies on detonation initiation by an imploding detonation wave, such as the third transition process [32–35]. Jackson and Shepherd [36] and Jackson et al. [37] designed an initiator for creating a collapsing toroidal detonation wave front and showed chemiluminescence images of the collapsing toroidal wave front concentrating at the central axis of the initiator.

Previous research by Wakita et al. [24] revealed that the transition from the incident planar detonation wave (Fig. 3a) to an expanding cylindrical detonation wave (Fig. 3b) in the first transition process is a sufficient condition for successful detonation wave propagation in the detonation chamber. Successful transition to the expanding cylindrical detonation wave (Fig. 3b) occurs when the predetonator diameter d is larger than 6.3λ and the reflecting board distance w equals the predetonator diameter d.

Preliminary Design of the Initiator

This section describes the preliminary design of the initiator when we use a stoichiometric hydrogen–oxygen mixture as a driver gas. As mentioned in the preceding section, a successful transition to an expanding cylindrical detonation wave (Fig. 4b) is a sufficient condition for a successful transition to a planer detonation wave in the detonation chamber. It is reasonable to assume that overfilling the upstream of the reflecting board with driver gas, as Fig. 1d shows, will ensure the initiation of an expanding cylindrical detonation wave in the detonation chamber. From this consideration, we chose the predetonator diameter d and the reflecting board clearance w to be seven times the cell size λ of the driver gas, being larger than the critical value of 6.3λ, which was described in the preceding section. The cell size λ of a stoichiometric hydrogen–oxygen driver mixture is about 1.2 to 1.3 mm at ambient pressure. Therefore, we chose the predetonator diameter d and the reflecting board clearance w to be 10 mm. The overfilling distance of the driver gas in this initiator, sufficient for a successful transition, is expected to be 10 mm, which is the same value as the reflecting board clearance w. The gap of the annular path L and the thickness of the board were 10 and 5 mm, respectively.

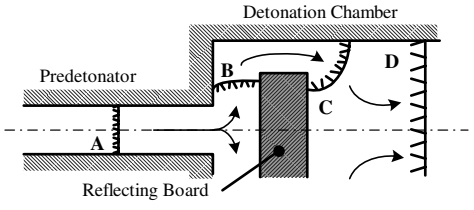

Fig. 4 Transition of detonation waves.

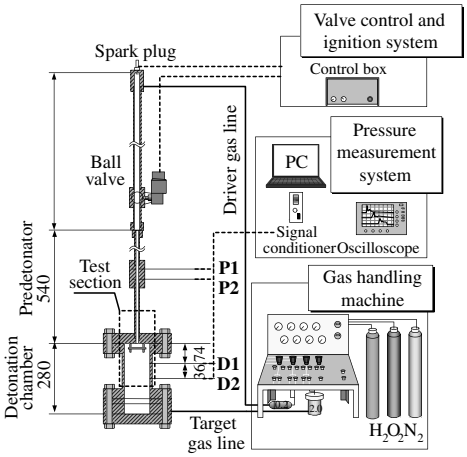

Fig. 5 Experimental apparatus.

Experimental Details

Experimental Apparatus

Figure 5 shows a schematic of the experimental apparatus. It consists mainly of a detonation chamber and a predetonator. The detonation chamber is 280 mm long, with an internal diameter of 100 mm. The predetonator upstream of the detonation chamber is 540 mm long, with an internal diameter of 10 mm. This length is sufficiently long compared with the DDT length of a stoichiometric hydrogen–oxygen mixture for this tube diameter. Four shafts support the reflecting board, which is 80 mm in diameter and 5 mm thick, as Figs. 2 and 5 show. As the preceding section describes, we chose the reflecting board clearance w, based upon the cell size of the driver gas, to be 10 mm. This apparatus has four ports P1, P2, D1, and D2, as shown in Fig. 5, for pressure sensors (PCB 113A26, Piezotronics Co., Ltd.). Soot foils collect tracks of the triple points of detonation waves at the following four locations in Fig. 6: location I is the surface of the front flange, location II is the upstream surface of the reflecting board, location III is the downstream surface of the reflecting board, and location IV is the sidewall of the detonation chamber.

Overfilling Procedure and Experimental Condition

To overfill the driver gas in the combustion chamber, an additional volume was installed in the upstream of the predetonator, as Fig. 5 shows. The additional volume is a 1 in. internal diameter tube and is connected with the predetonator via a ball valve. Figure 7 shows the overfilling procedure. Initially, the valve is closed and the driver gas mixture and the target gas mixture fill the upstream and downstream areas of the valve, respectively (Fig. 7a). A gas-handling machine prepares and completely mixes these mixtures. The pressure of the driver gas p_1 is higher than that of the target gas p_2. When the valve opens (Fig. 7b), the driver gas overfills to the position h where the balance pressure p_3 is established. Common to all experiments, the balance pressure (initial pressure) is 1 atm. A control device determines the timing of the valve opening and ignition, and it

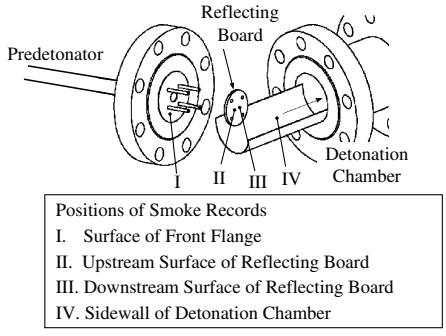

Fig. 6 Positions of soot foils.

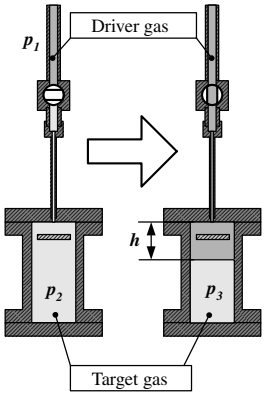

a) Valve close b) Valve open

Fig. 7 Overfilling procedure.

activates a spark plug 0.5 s after the valve opens. A characteristic overfilling distance h_c serves as a criterion of the driver gas amount: The distance h_c is the overfilling volume of the driver gas at the initial pressure divided by the cross-sectional area of the detonation chamber. Note that the actual overfilling distance can be different from h_c because of the volume of the reflecting board. In all cases, the driver gas and the target gas are stoichiometric hydrogen–oxygen and stoichiometric hydrogen–air mixtures, respectively. The maximum value of the differential pressure $(p_1 - p_2)$ in the present study is about 1.3 atm at $h_c = 30$ mm.

Results and Discussion

Performance Confirmation of Preliminary Design

Filling the driver gas mixture (stoichiometric hydrogen–oxygen mixture) into the entire test section, we checked the initiator performance. Figure 8 shows pressure histories at ports P1 to D2 for the same experiment. All of the pressure histories exhibit a rapid pressure rise. The time lags of the steep pressure rises of P1–P2 and D1–D2 give velocities of 2.9 and 3.0 km/s, respectively. These values are close to the theoretical Chapman–Jouguet (CJ) detonation velocity of 2.8 km/s under a stoichiometric hydrogen–oxygen mixture. Accordingly, a CJ detonation wave is transmitted along the axis in the predetonator and the combustion chamber.

Figure 9 shows soot tracks, and Fig. 10 shows a detonation transition diagram based on the soot tracks. Figure 9a shows the soot track of the front flange surface. The diameter of this soot track is 100 mm, which is the same as the diameter of the detonation chamber. In the left figure, the central white circle is the predetonator exit, and the four surrounding circles correspond to the support shafts. An annular black ring surrounds the predetonator exit. The detonation cell patterns extend outside the black ring, as the close up in the right figure shows. Figure 9b shows the soot track of the upstream surface of the reflecting board. The four white circles correspond to the support shafts again. The cell pattern suggests a detonation wave propagating radially from the center of the reflecting board. As Fig. 10 shows, the incident planar detonation wave diffracts at the exit of the predetonator and is weakened by the expansion wave from the edge of the predetonator. As a result, the incident detonation wave cannot attenuate longer than this reflecting board clearance. At the center of the reflecting board, the detonation wave recommences and spreads back to the front flange. The annular black ring of the front flange surface corresponds to the interface between the diffracted shock from the predetonator and the detonation wave from the reflecting board. The detonation wave from the reflecting board collides with the front flange surface. This collision strengthens the detonation wave propagating in the radial direction, as the dashed–dotted line in the figure shows. This is the reason the cell size on the reflecting board (Fig. 9a) is bigger than that on the front flange (Fig. 9b). In this way, an expanding cylindrical detonation wave evolves between the front flange and the reflecting board. Like a detonation wave emerging from a tube exit, the expanding cylindrical detonation wave emerges from the edge of the reflecting board and then comes under the influence of the rarefaction wave. Figure 9d shows the soot track of the sidewall of the detonation chamber. The size of the track is 700×1700 mm, and the front flange is at the left end. The axial position of the reflecting board is

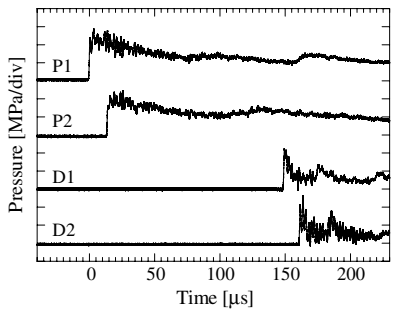

Fig. 8 Pressure history when filling driver gas mixture (stoichiometric hydrogen–oxygen mixture) into entire test section.

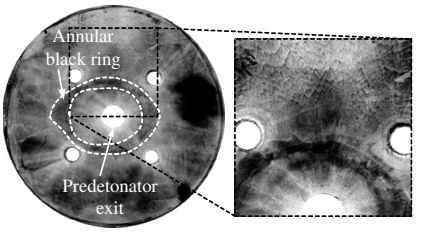

a) Surface of front flange (location II in Fig. 6)

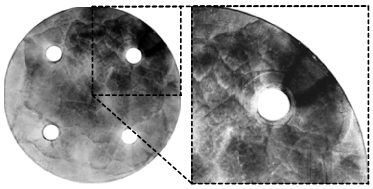

b) Upstream surface of reflecting board (location III in Fig. 6)

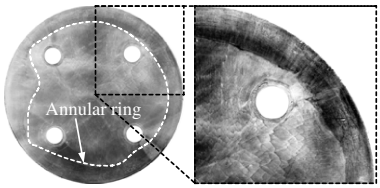

c) Downstream surface of reflecting board (location IV in Fig. 6)

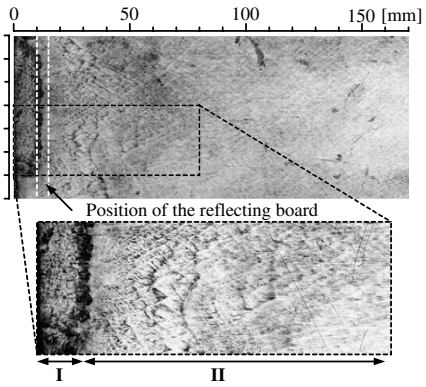

d) Sidewall of detonation chamber (location V in Fig. 6)

Fig. 9 Soot tracks when filling driver gas mixture only.

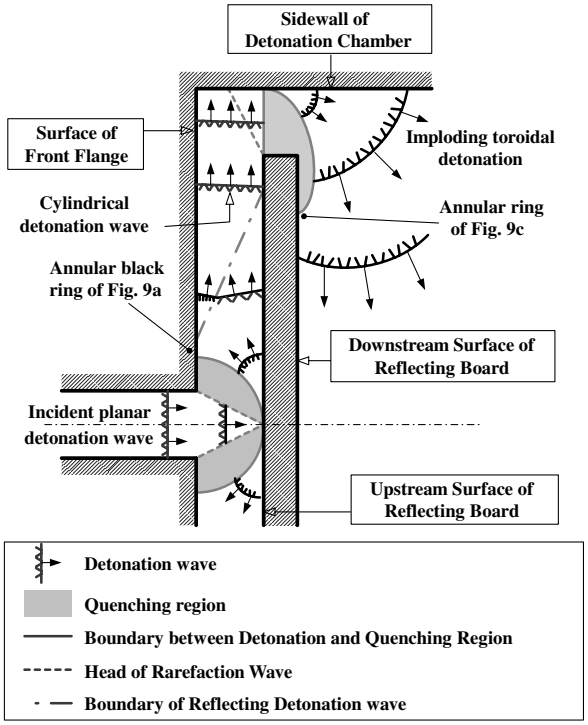

Fig. 10 Schematic diagram of detonation transition around reflecting board.

from 10 to 15 mm from the left end. As location 1 in Fig. 9d shows, the expanding cylindrical detonation wave emerging from the edge of the reflecting board collides with the sidewall at a zonal area. The width of this zonal area is approximately 12 mm, being close to the reflecting board clearance $w = 10$ mm. Because the cell size λ of a stoichiometric hydrogen–oxygen mixture is about 1.2 to 1.3 mm at ambient pressure, the distance between the edge of the reflecting board and the front flange (namely, the reflecting board clearance) corresponds to 8–9λ. In a cross-sectional surface, Fig. 10 shows the expanding cylindrical detonation wave diffracts only from the edge of the reflecting board to the left, as the dashed line in the figure shows. An earlier study revealed that, when a detonation wave transits from a rectangular channel to an unconfined space, the critical width of the flow channel is 10λ [10]. Compared with the half value of 10λ, the value of 8–9λ is large enough for the expanding cylindrical detonation wave to survive the rarefaction waves. The expanding cylindrical wave keeps its strength while it passes over the gap in the annular path L and causes a strong reflection on the sidewall (location I in Fig. 9d). At the left end of location II in Fig. 9d, comparatively small cells are observable, showing evidence of overdriven detonation. This result shows that the strong reflection of the expanding cylindrical detonation wave caused a successful reinitiation of an imploding toroidal detonation wave (Fig. 4b). Figure 9c is the soot track on the downstream surface of the reflecting board. In this figure, an annular ring divides the surface into the inner area and the outer area. Cell patterns observable in the inner area show the imploding toroidal detonation wave diffracted to the downstream surface of the reflecting board, as Fig. 10 shows. Not only the pressure history but also the soot track pattern prove the successful transition of the detonation.

Notable results of this performance confirmation test are as follows:

1) We obtained a successful transition of a detonation wave by setting the predetonator diameter d, the reflecting board clearance w, and the gap of the annular path L to 10 mm. Note that this predetonator diameter d is below the classical critical diameter of 13λ, meaning 16 to 17 mm for a stoichiometric hydrogen–oxygen mixture.

2) All three transitions around the reflecting board, such as a planer wave to an expanding cylindrical wave, the expanding cylindrical wave to an imploding toroidal wave, and the imploding toroidal wave to a planar wave, were successful.

Detonation Transition Using the Overfilling Method

By using the overfilling method, we examined the detonation transitions around the reflecting board by changing the characteristic overfilling distance h_c. The driver gas mixture and the target gas mixture are a stoichiometric hydrogen–oxygen mixture and a stoichiometric hydrogen–air mixture, respectively. Figure 11 shows soot tracks with a characteristic overfilling distance h_c of 10 mm, which is the same length as the reflecting board clearance $w =$ 10 mm. Although cell patterns appear around part of a shaft, as Fig. 11a shows, this pattern is quite different from that of Fig. 9a. No cell pattern is observable on the upstream surface of the reflecting board, as Fig. 11b shows. Accordingly, the detonation reinitiation did not occur on the reflecting board, resulting in the failure of the detonation transition to the detonation chamber in this condition. A possible cause of this result is the lower quality driver gas in the upstream of the reflecting board due to the mixing of the driver gas and target gas. Our overfilling method, shown in Fig. 7, has a mixing effect on the driver gas and the target gas at the contact surface during the period the valve is open to ignition. Therefore, the concentration of nitrogen at the leading edge of the driver gas likely rises at the end of the overfilling procedure. Preparing an uncontaminated driver gas mixture in the upstream of the reflecting board is crucial to developing an expanding cylindrical detonation wave under this experimental condition.

Figure 12 shows soot tracks with a characteristic overfilling distance h_c of 20 mm. There is an annular black ring on the surface of the front flange (Fig. 12a), just like in Fig. 9a. Figure 12b shows the cell patterns of a detonation wave propagating radially in the area outside the ring. These results prove a successful transition from a planar detonation wave in the predetonator to an expanding cylindrical detonation wave between the front flange and the reflecting board. The influence of the four shafts to the detonation transition was not observed in the cell patterns, because the cylindrical detonation wave reinitiates the inner region of the bolt radius and the detonation wave spreads before the influence reaches the entire circumference. On the sidewall of the detonation chamber (location I in Fig. 12c), there is a zonal area, at which point the expanding cylindrical detonation wave vertically collides with the sidewall. The width of the zonal area is approximately 10 mm, which is close to the width that location I in Fig. 9d shows. Accordingly, the expanding cylindrical detonation wave survived the rarefaction wave from the edge of the reflecting board and reached the sidewall, just as the transition in Fig. 10 describes. However, as location II in Fig. 12c shows, no cell pattern is observable in the right side of the zonal area, meaning that the transition from the expanding cylindrical detonation wave to an imploding toroidal detonation wave failed.

Figure 13 shows soot tracks with a characteristic overfilling distance h_c of 30 mm. The soot tracks around the reflecting board show similar patterns to those in Fig. 12. The incoming planar detonation wave transmitted to an expanding cylindrical detonation wave successfully, and the expanding cylindrical wave reached the sidewall. Unfortunately, the imploding toroidal detonation wave did

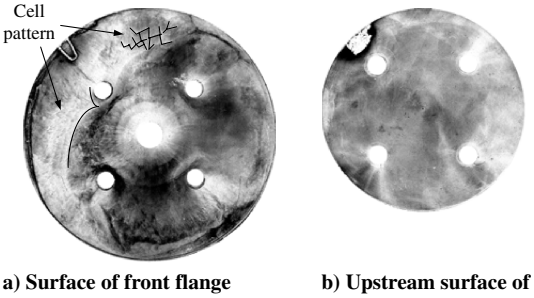

a) Surface of front flange (location II in Fig. 6) **b) Upstream surface of reflecting Board (location III in Fig. 6)**

Fig. 11 Soot tracks with characteristic overfilling distance $h_c =$ 10 mm.

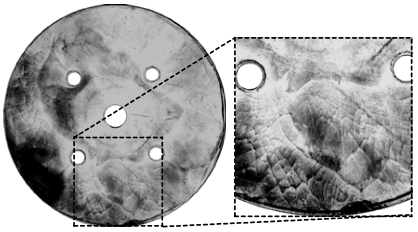

a) Surface of front flange (location II in Fig. 6)

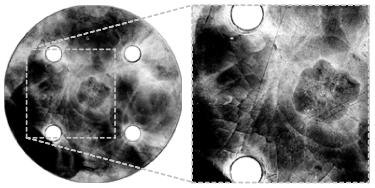

b) Upstream surface of reflecting board (location III in Fig. 6)

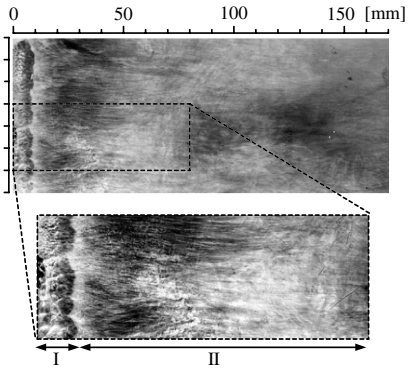

c) Sidewall of detonation chamber (location V in Fig. 6)

Fig. 12 Soot tracks with characteristic overfilling distance h_c= 20 mm.

not commence on the sidewall. However, unlike the h_c of the 20 mm case, the detonation cell structure reappeared on the downstream half of the combustion chamber sidewall as the bottom, right close up in Fig. 13d shows. Figure 14 shows pressure histories at ports P1 to D2 for this experiment. Because ports D1 and D2 are 74 and 110 mm, respectively, from the left end of the soot track in Fig. 13d, the location of the detonation reappearance is between these two ports. At port D1, the history shows a small oscillation continuing for about 30 μs before the rapid pressure increase and, at port D2, the history also appears to be a small pressure oscillation, showing that a decaying shock wave passed through ports D1 and D2. The time lag between the small pressure oscillations of these two ports is about 21 μs. This time lag gives the velocity of the pressure wave from ports D1 to D2 to be 1.7 km/s, which is considerably larger than the speed of sound under a stoichiometric hydrogen–air mixture. This decaying shock does not spread along the sidewall of the detonation chamber but would have spread from the center of the chamber. Cell patterns near the location of the detonation reappearance are irregular, which is the characteristic appearance of a soot track when a detonation wave collides vertically with a soot foil. The time lag between the rapid pressure increases of these two ports is about 10 μs. This time lag gives the velocity of the pressure wave from ports D1 to D2 to be 3.6 km/s, which is considerably larger than the theoretical CJ detonation velocity of 2.0 km/s under a stoichiometric hydrogen–air mixture. Soot tracks and pressure histories in Figs. 13 and 14 lead to a detonation reinitiation mechanism, as Fig. 15 shows. The expanding cylindrical detonation wave fails to transit to an imploding toroidal detonation wave, and a torus-shaped compression wave encompasses the combustible gas in the detonation chamber. This torus-shaped pressure wave concentrates at the

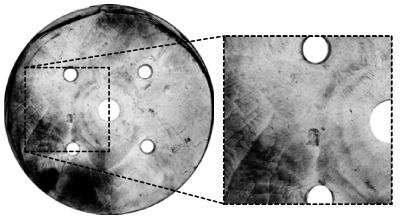

a) Surface of front flange (location II in Fig. 6)

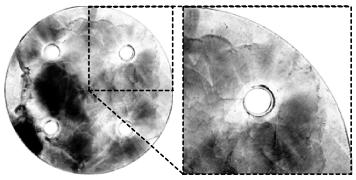

b) Upstream surface of reflecting board (location III in Fig. 6)

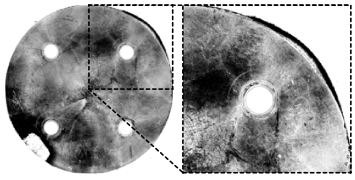

c) Downstream surface of reflecting board (location IV in Fig. 6)

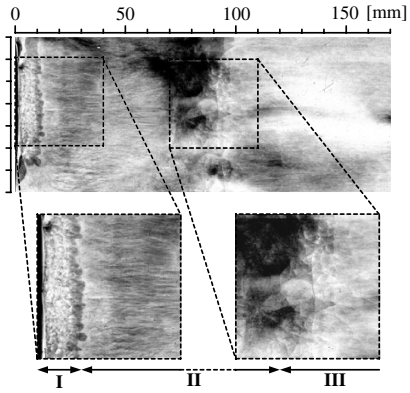

d) Sidewall of detonation chamber (location V in Fig. 6)

Fig. 13 Soot tracks with characteristic overfilling distance h_c= 30 mm.

axis of the detonation chamber behind the reflecting board, generating a region of high temperature and high pressure sufficient for detonation reinitiation. A hemispherical detonation wave evolving from this region propagates and reaches ports D1 and D2 with a small temporal difference.

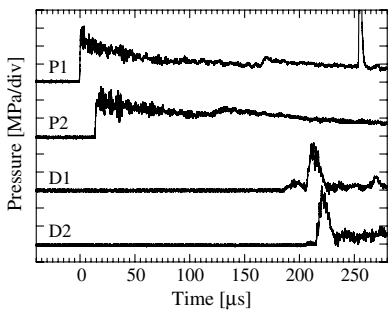

Fig. 14 Pressure history with characteristic overfilling distance h_c= 30 mm.

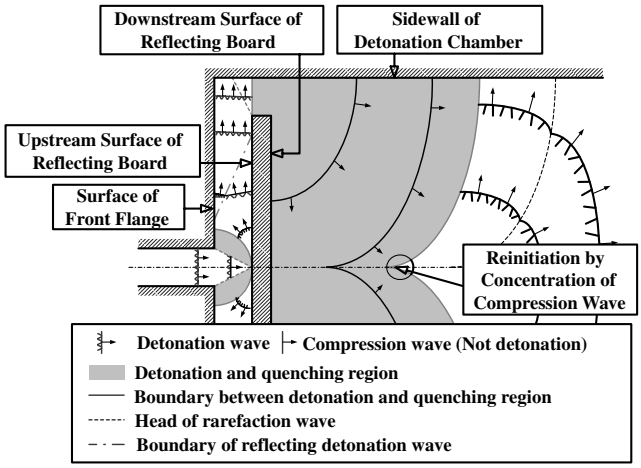

Fig. 15 Schematic diagram of detonation reinitiation mechanism with characteristic overfilling distance $h_c = 30$ mm.

Owing to this mechanism, a successful detonation transition is possible, even in a case where the expanding cylindrical detonation wave fails to transit to an imploding toroidal detonation wave. The nitrogen concentration resulting from the mixing effect around the reflecting board affects the probability of a successful detonation transition. In the condition of $h_c = 30$ mm, the nitrogen concentration around the reflecting board is low compared with the $h_c =$ 20 mm case. As a result, the pressure after the compression wave increases, resulting in the improvement of the reinitiation probability behind the reflecting board. These experimental results prove that the transition from a expanding cylindrical detonation wave to an imploding toroidal detonation wave is not a necessary condition, but the transition to an imploding toroidal shock is likely a necessary condition for successful detonation initiation in a detonation chamber filled with a target gas. They also prove that the minimum characteristic overfilling distance h_c of this detonation initiator is 30 mm.

Although a successful detonation initiation in the detonation chamber is possible without a transition from an expanding cylindrical wave to an imploding toroidal wave, interruption of detonation propagation during a transition process is unfavorable for the operation frequency because of the decrease in flame propagation velocity. Accordingly, it is important to avoid the mixing effect of the driver gas and the target gas around the reflecting board to ensure a successful transition from an expanding cylindrical detonation wave to an imploding toroidal detonation wave. Figure 16 shows a schematic diagram of driver gas overfilling around the reflecting board with a characteristic overfilling distance h_c of 30 mm. As shown in Fig. 16, assuming that the driver gas overfilled from the annular orifice around the reflecting board spread like a cylindrical shape, the distance of the leading edge of the cylinder is represented as $w + (h_c - w) \times (A_{\text{chamber}}/A_{\text{orifice}})$. A_{chamber} is the area of the detonation chamber cross section, and A_{orifice} is area of the annular orifice. From this relation, the driver gas flows into the detonation

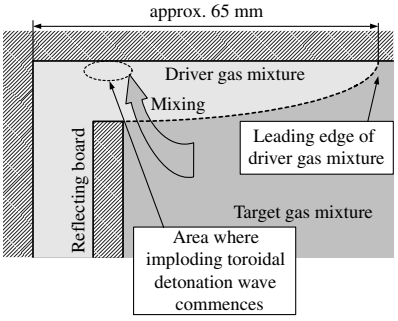

Fig. 16 Schematic diagram of driver gas overfilling around reflecting board with characteristic overfilling distance $h_c = 30$ mm.

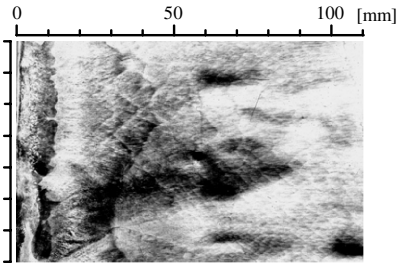

Fig. 17 Soot tracks on sidewall. Length of reflecting board set to 100 mm. Characteristic overfilling distance $h_c = 17.2$ mm.

chamber along the sidewall, and the leading edge of the driver gas can reach as far as 66 mm from the front wall. Therefore, the mixing effect at the leading edge of the driver gas is unlikely to result in an increase in nitrogen concentration at the origin of the imploding toroidal detonation wave (see Fig. 16).

A possible cause of the increase in nitrogen concentration at this region is the inflow of the target gas from rearward of the reflecting board, as Fig. 16 shows. To confirm this effect, we increased the thickness of the reflecting board from 5 to 100 mm and conducted similar experiments. Figure 17 shows the soot track on the sidewall with a characteristic overfilling distance h_c of 17.2 mm. The size of the track is 700×1100 mm, and the right end corresponds to the downstream end of the new reflecting board. In this figure, we can see cell structures at 10 mm from the left as evidence of a reinitiation of an imploding toroidal detonation with such a short overfilling distance. Accordingly, the characteristic overfilling distance h_c to have an imploding toroidal detonation wave is less than 17.2 mm when using a reflecting board with an appropriate thickness. The fact that there is a case of a successful detonation transition into the detonation chamber, even when the transition to an imploding toroidal detonation wave is unsuccessful ($h_c = 30$ mm case), shows that an imploding toroidal detonation wave formation is a sufficient condition to have a planar detonation wave propagate in the detonation chamber.

Comparing Fig. 1b with Fig. 1d, the reduction effect of the reflecting board on the overfilling distance is estimated with regard to our detonation chamber of 100 mm ID. A previous study by Wakita et al. confirmed that the critical tube diameter of the predetonator without a reflecting board was 20 mm when a stoichiometric hydrogen–oxygen driver gas mixture at atmospheric pressure fills an entire section [24]. In view of the fact that the cell size of this initial condition is about 1.2–1.3 mm, it is appropriate to consider the critical diameter to be 20 mm from the relation of $D_c = 13\lambda$. Figure 18 shows the soot tracks on the sidewall of the detonation chamber in this condition. The track is 70×170 mm, and the

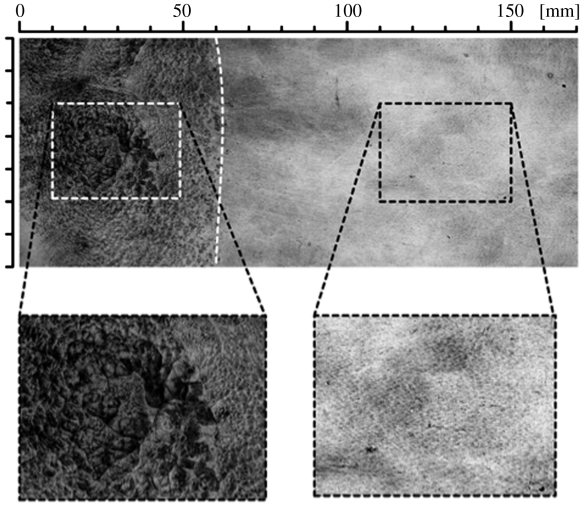

Fig. 18 Soot tracks on sidewall of detonation chamber without reflecting board (predetonator diameter $d = 20$ mm).

predetonator exit is at the left end. The predetonator diameter is increased to 20 mm to satisfy the 13λ criterion. At 60 mm from the left end, there is a boundary between two different soot track patterns. A spherical detonation wave reinitiated at the predetonator exit and collided with the upstream of the boundary vertically. In the downstream of the boundary, a complete planar detonation wave was established. For these reasons, we can identify the point as a transition point from the expanding spherical detonation to the planar detonation wave. We assume that the planar detonation wave of the driver gas passing through the circular tube with the constant section is able to transmit to the target gas composition. This result shows that the minimum overfilling distance without a reflecting board, which is shown as $\boldsymbol{h}$ in Fig. 1b, is 60 mm. However, when we overfill a driver gas mixture of hydrogen–oxygen for any overfilling distance using our method, we could not observe a successful transition. This is because our method cannot substitute the target gas in the upstream of the detonation chamber perfectly with the driver gas. Part of the target mixture remains after the overfilling procedure at the upstream corner of the detonation chamber. Additionally, mixing of the driver mixture and the target mixture occurs at the leading edge of the driver mixture. By using a reflecting board, as shown in Fig. 1d, the characteristic overfilling distance $\boldsymbol{h}_c$ required to have a planar detonation wave propagate in the detonation chamber decreases to 17.2 mm. Accordingly, a reflecting board with an appropriate thickness not only solves the difficulty in substituting the gas in the upstream of the detonation chamber, it also reduces the driver gas overfilling distance $\boldsymbol{h}$.

Conclusions

A detonation wave propagates around the reflecting board, changing its shape through three transition processes: from planer to cylindrical, toroidal, and back to planar again. Inspired by our previous result, that showed the transition to an expanding cylindrical detonation wave is a sufficient condition to have a planar detonation wave propagate in the detonation chamber successfully, the authors experimentally examined a combination method of a reflecting board and the overfilling of driver gas. A preliminary experiment with a stoichiometric hydrogen–oxygen mixture (cell size $\lambda = 1.2$ to 1.3 mm) showed that the appropriate values for the predetonator diameter and the reflecting board clearance are 10 mm for both. The diameter of 10 mm is half that for the case without a reflecting board. This means that the method reduces the amount of driver gas in the predetonator to one quarter. The advantage of the reflecting board that adjusts the amount of the driver gas to one quarter can be applied to all the fuel–air mixtures that satisfy the relational expression of 13λ that shows the critical tube diameter.

By using this initiator configuration, a successful transition to the detonation chamber is observed when the overfilling distance $\boldsymbol{h}_c$ is at least 30 mm. With an overfilling distance $\boldsymbol{h}_c$ of 30 mm, an expanding cylindrical detonation wave transforms, not to an imploding toroidal detonation wave, but to a torus-shaped pressure wave because of the mixing effect of the driver gas and the target gas around the reflecting board. The torus-shaped pressure wave concentrates at the axis of the detonation chamber behind the reflecting board, generating a region of high temperature and high pressure sufficient for detonation reinitiation.

Although the critical overfilling distance of 30 mm is small compared with the case without a reflecting board, this result is still far from its full potential. The nitrogen concentration resulting from the mixing effect around the reflecting board affects the probability of a successful transition from an expanding cylindrical detonation wave to an imploding toroidal wave. A reflecting board 100 mm thick prevents the effect of the inflow of the target gas from the rear of the reflecting board. As a result, a successful transition from an expanding cylindrical detonation wave to an imploding toroidal one becomes possible with a characteristic overfilling distance as small as 17.2 mm. Accordingly, the reflecting board makes the driver gas overfilling distance $\boldsymbol{h}$ at least three times smaller. As a common interpretation, the cylindrical to the toroidal detonation on the sidewall plays a vital role in the successful transition, and we must prevent the mixing effect completely at the reinitiation position of the toroidal detonation wave.

Acknowledgment

This research is partially supported by the Japan Society for the Promotion of Science Grants-in-Aid for Young Scientists (B) (KAKENHI) (21760646).

References

[1] Nicholls, J. A., Wilkinson, H. R., and Morrison, R. B., "Intermittent Detonation as a Thrust-Producing Mechanism," *Jet Propulsion*, Vol. 27, No. 5, 1957, pp. 534–541.

[2] Kailasanath, K., "Review of Propulsion Applications of Detonation Waves," *AIAA Journal*, Vol. 38, No. 9, 2000, pp. 1698–1708. doi:10.2514/2.1156

[3] Kailasanath, K., "Recent Developments in the Research on Pulse Detonation Engines," *AIAA Journal*, Vol. 41, No. 2, 2003, pp. 145–159. doi:10.2514/2.1933

[4] Roy, G. D., Frolov, S. M., Borisov, A. A., and Netzer, D. W., "Pulse Detonation Propulsion: Challenges, Current Status, and Future Perspective," *Progress in Energy and Combustion Science*, Vol. 30, No. 6, 2004, pp. 545–672. doi:10.1016/j.pecs.2004.05.001

[5] Kaneshige, M., and Shepherd, J. E., "Detonation Database," Graduate Aerospace Laboratories of the California Inst. of Technology TR FM97-8, Pasadena, CA, 1997.

[6] Helman, D., Shreeve, R. P., and Eidelman, S., "Detonation Pulse Engine," AIAA Paper 1986-1683, June 1986.

[7] Edwards, D. H., Thomas, G. O., and Nettleton, M. A., "The Diffraction of a Planar Detonation Wave at an Abrupt Area Change," *Journal of Fluid Mechanics*, Vol. 95, No. 1, 1979, pp. 79–96. doi:10.1017/S002211207900135X

[8] Shepherd, J. E., Schultz, E., and Akbar, R., "Detonation Diffraction," *Proceedings of the Twenty-Second International Symposium on Shock Waves*, Vol. 1, Southampton Univ. Media, Southampton, U. K., 2000, pp. 41–48.

[9] Pitgen, F., and Shepherd, J. E., "Detonation Diffraction in Gases," *Combustion and Flame*, Vol. 156, No. 3, March 2009, pp. 665–677. doi:10.1016/j.combustflame.2008.09.008

[10] Mitrofanov, V. V., and Soloukhin, R. I., "The Diffraction of Multifront Detonation Waves," *Soviet Physics, Doklady*, Vol. 9, No. 12, 1965, pp. 1055–1058.

[11] Matsui, H., and Lee, J. H., "On the Measure of the Relative Detonation Hazards of Gaseous Fuel–Oxygen and Air Mixtures," *Proceedings of 17th Symposium (International) on Combustion*, Combustion Inst., Pittsburgh, 1978, pp. 1269–1280.

[12] Knystautas, R., Lee, J. H., and Guirao, C. M., "The Critical Tube Diameter for Detonation Failure in Hydrocarbon–Air Mixtures," *Combustion and Flame*, Vol. 48, No. 1, 1982, pp. 63–83. doi:10.1016/0010-2180(82)90116-X

[13] Schultz, E., "Detonation Diffraction Through an Abrupt Area Expansion," Ph.D. Thesis, California Inst. of Technology, Pasadena, CA, April 2000.

[14] Moen, O., Funk, J. W., Ward, S. A., Rude, M. G., and Thibault, P. A., "Detonation Length Scales for Fuel–Air Explosives," *Progress in Astronautics and Aeronautics*, Vol. 94, AIAA, New York, 1983, pp. 55–79.

[15] Moen, I. O., Sulmistras, A., Thomas, G. O., Bjerketvedt, D., and Thibault, P. A., "Influence Of Cellular Regularity On The Behavior Of Gaseous Detonations," *Progress in Astronautics and Aeronautics*, Vol. 106, AIAA, New York, 1986, pp. 220–243.

[16] Shepherd, J. E., Moen, I. O., Murray, S. B., and Thibault, P. A., "Analysis of the Cellular Structure of Detonations," *Proceedings of the 21th Symposium (International) on Combustion*, Combustion Inst., Pittsburgh, 1986, pp. 1649–1658.

[17] Desbordes, D., "Transmission Of Overdriven Plane Detonations: Critical Diameter as a Function of Cell Regularity and Size," *Progress in Astronautics and Aeronautics*, Vol. 114, AIAA, Washington, D. C., 1988, pp. 170–185.

[18] Desbordes, D., Guerraud, C., Hamada, L., and Presles, H. N., "Failure of the Classical Dynamic Parameters Relationships in Highly Regular Cellular Detonation Systems," *Progress in Astronautics and Aeronautics*, Vol. 153, AIAA, Washington, D. C., 1993, pp. 347–359.

[19] Aamio, M. J., Hinkey, J. B., and Bussing, T. R. A., "Multiple Cycle Detonation Experiments During the Development of a Pulse Detonation Engine," AIAA Paper 1996-3263, 1996.

[20] Brophy, C. M., Netzer, D. W., Sinibaldi, J., and Johnson, R., "Detonation of A JP-10 Aerosol for Pulse Detonation Application," *High-Speed Deflagration and Detonation*, Elex-KM Publ., Moscow, 2001.

[21] Moen, I. O., Sulmistras, A., Thomas, G. O., Bjerketvedt, D., and Thibault, P. A., "Influence of Cellular Regularity on the Behaviour of Gaseous Detonations," *Progress in Astronautics and Aeronautics*, Vol. 106, AIAA, New York, 1968, pp. 220–243.

[22] Sorin, R., Zitoun, R., Khasainov, B., and Desbordes, D., "Detonation Diffraction Through Different Geometries," *Shock Waves*, Vol. 19, No. 1, 2009, pp. 11–23. doi:10.1007/s00193-008-0179-1

[23] Khasainov, B., Presles, H. N., Desbordes, D., Demontis, P., and Vidal, P., "Detonation Diffraction from Circular Tubes To Cones," *Shock Waves*, Vol. 14, No. 3, 2005, pp. 187–192. doi:10.1007/s00193-005-0262-9

[24] Wakita, M., Numakura, R., Itoh, Y., Sugata, S., Totani, T., and Nagata, H., "Detonation Transition Limit at an Abrupt Area Change Using a Reflecting Board," *Journal of Propulsion and Power*, Vol. 23, No. 2, 2007, pp. 338–344. doi:10.2514/1.24421

[25] Wakita, M., Numakura, R., Ito, Y., Nagata, H., Totani, T., and Kudo, I., "Re-Initiation Mechanisms of a Detonation Wave in the PDE Initiator Using a Reflecting Board," *Journal of the Japan Society for Aeronautical and Space Sciences*, Vol. 53, No. 621, 2005, pp. 414–418 (in Japanese).

[26] Teodorczyk, A., Lee, J. H. S., and Knystautas, R., "Propagation Mechanism of Quasi-Detonations," *Proceedings of 22nd Symposium (International) on Combustion*, Combustion Inst., Pittsburgh, 1988, pp. 1723–1731.

[27] Jones, D. A., Sichel, M., and Oran, E. S., "Reignition of Detonations by Reflected Shocks," *Shock Waves*, Vol. 5, Nos. 1–2, 1995, pp. 47–57. doi:10.1007/BF02425035

[28] Ohyagi, S., Obara, T., Hoshi, S., Cai, P., and Yoshihashi, T., "Diffraction and Re-Initiation of Detonations Behind a Backward-Facing Step," *Shock Waves*, Vol. 12, No. 3, 2002, pp. 221–226. doi:10.1007/s00193-002-0156-z

[29] Murray, S. B., and Lee, J. H., "On the Transformation of Planar Detonation to Cylindrical Detonation," *Combustion and Flame*, Vol. 52, No. 3, 1983, pp. 269–289. doi:10.1016/0010-2180(83)90138-4

[30] Murray, S. B., Thibault, P. A., Zhang, F., Bjerketvedt, D., Sulmistras, A., Thomas, G. O., Jenssen, A., and Moen, I. O., *High-Speed Deflagration and Detonation: Fundamentals and Control*, edited by G. D. Roy, S. M. Frolov, D. Netzer, and A. A. Borisov, Elex-KM Publ., Moscow, 2001, pp. 139–162.

[31] de Witt, B., Ciccarelli, G., Zhang, F., and Murray, S., "Shock Reflection Detonation Initiation Studies for Pulse Detonation Engines," *Journal of Propulsion and Power*, Vol. 21, No. 6, 2005, pp. 1117–1125. doi:10.2514/1.14398

[32] Jackson, S. I., and Shepherd, J. E., "A Toroidal Imploding Detonation Wave Initiator for Pulse Detonation Engines," *AIAA Journal*, Vol. 45, No. 1, 2007, pp. 257–270. doi:10.2514/1.24662

[33] Jackson, S. I., and Shepherd, J. E., "Detonation Initiation in a Tube via Imploding Toroidal Shock Waves," *AIAA Journal*, Vol. 46, No. 9, 2008, pp. 2357–2367. doi:10.2514/1.35569

[34] Wang, B., He, H., and Yu, S.-T., "Direct Calculation of Wave Implosion for Detonation Initiation," *AIAA Journal*, Vol. 43, No. 10, 2005, pp. 2157–2169. doi:10.2514/1.11887

[35] Li, C., and Kailasanath, K., "Detonation Initiation by Annular-Jet-Induced Imploding Shocks," *Journal of Propulsion and Power*, Vol. 21, No. 1, 2005, pp. 183–186. doi:10.2514/1.5463

[36] Jackson, S. I., and Shepherd, J. E., "Initiation Systems for Pulse Detonation Engines," AIAA Paper 2002-3627, 2002.

[37] Jackson, S. I., Grunthaner, M. P., and Shepherd, J. E., "Wave Implosion as an Initiation Mechanism for Pulse Detonation Engine," AIAA Paper 2003-4820, 2003.

J. Powers
Associate Editor